

## Conference Paper

# Softened Variable Angle Truss Model (RA-STM): Model Description and Refinement/Optimization Proposals

Benedito Filho<sup>1</sup>, Luís Bernardo<sup>1</sup>, and Bernardo Horowitz<sup>2</sup><sup>1</sup>C-MADE - Centre of Materials and Building Technologies, University of Beira Interior, Covilhã, Portugal<sup>2</sup>Department of Civil Engineering, Federal University of Pernambuco, Brazil

## Abstract

This article presents a recent softened truss model with variable angle, namely the refined RA-STM (Rotating-Angle Softened Truss Model), to model the behaviour of structural concrete plates under pure shear. The equations of the model, as well as the solution procedure, are summarized. Some predictions from the RA-STM are also presented, discussed and compared with experimental results available in the literature. It is shown that the refined RA-STM still needs to be refined. In addition, the need to generalize the RA-STM for more general loading cases is also discussed as well as the need to optimize the solution procedure in order to facilitate its computational implementation.

Corresponding Author:

Benedito Filho

benedito.madian.filho@ubi.pt

Received: 7 January 2020

Accepted: 21 April 2020

Published: 3 May 2020

Publishing services provided by  
Knowledge E

© Benedito Filho et al. This article is distributed under the terms of the [Creative Commons Attribution License](#), which permits unrestricted use and redistribution provided that the original author and source are credited.

Selection and Peer-review under the responsibility of the STARTCON19 Conference Committee.

## 1. Introduction

It is a common practice in structural engineering to discretize complex structures as a combination of simpler elements. As shown in Fig. 1 (a), some structures can be idealized as a set of two-dimensional structural concrete elements (panels, plates or membranes), with the reinforcement rebars usually arranged in orthogonal directions. Such elements are only subjected to in-plane stresses, which generate internal membrane forces. The full behaviour of such elements can be predicted with softened truss models (STM) considering rotating angles (RA) for the struts. Such models are called softened variable angle truss models or rotating angle – soft truss models (RA-STM).

Simple computational tools can be created from such models, which can be very useful to help for the design of structural concrete structures, namely to check the local safety of membrane elements.

The implementation of these nonlinear models is usually made in computers by using softwares with programming languages, such as MATLAB [1]. This allows to assess, calibrate and modify such models more easily.

## OPEN ACCESS

## 2. Description of the RA-STM Model

The RA-STM model was proposed by Belarbi and Hsu in 1994 [2] and Pang and Hsu in 1995 [3]. Recently, this model has been refined by Silva and Horowitz in 2015 [4], Silva in 2016 [5], Cerquido in 2017 [6] and Bernardo *et al.* in 2018 [7, 8].

The resistance mechanism of RA-STM is assumed to be a plane truss, in which the concrete resists to compressive stresses and the reinforcement resists to tensile stresses (Fig. 1 (b)). The non-linear behaviour and the softening effect of concrete are key features of this model. This model is based on the three Navier's principles of material mechanics, namely: stresses equilibrium, strains compatibility and constitutive relationships for the materials.

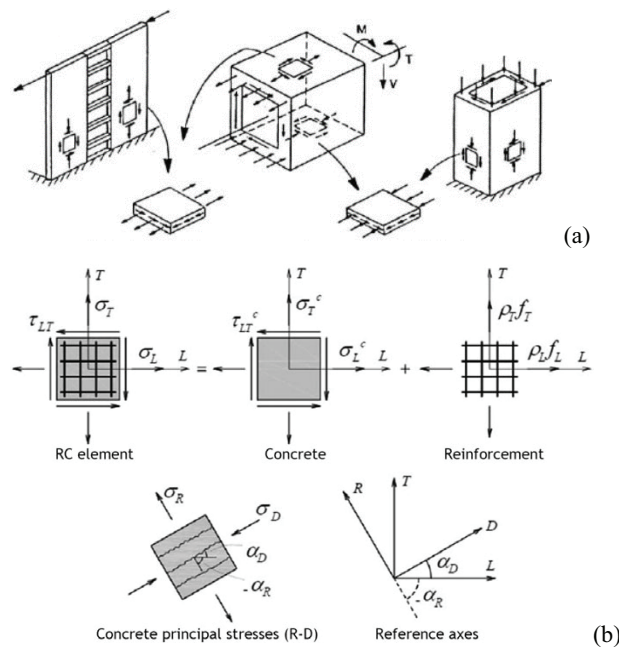


**Figure 1:** Membrane elements to analyse concrete structures [5, 6].

In the RA-STM, the equations derived from the stresses equilibrium and strains compatibility are obtained through the analysis of the Mohr's circle for stresses ( $\sigma$ ) and strains ( $\epsilon$ ), while the constitutive relationships for concrete and steel are assumed and based on average  $\sigma - \epsilon$  relationships experimentally calibrated and found in the literature. For this reason, the relationship for concrete in compression ( $\sigma_D - \epsilon_D$ ) in the principal direction of stresses has two main characteristics: a nonlinear relationship between stresses and strains and the influence of the softening effect in concrete due to transverse tensile stresses and diagonal cracking. For this latter, a softening coefficient  $\zeta$  is incorporated to the constitutive relationship for concrete, which is experimentally calibrated and based on proposals that can be found in the literature.

## 2.1. Equations for RA-STM

Tables 1 to 3 summarize the set of equations of RA-STM. Details about the derivation of the presented equations for the original RA-STM and for reinforced concrete (RC) panels can be found in previous studies [2, 3, 5–7]. The meaning of all parameters can be found in the notation list at the end of this article. Some parameters can also be visualized in Fig. 1 (b).

TABLE 1: Equilibrium and compatibility equations [2, 3].

| Equilibrium equations (stresses)  |  |     |
|---|--|-----|
| $\begin{bmatrix} \sigma_L \\ \sigma_T \\ \tau_{LT} \end{bmatrix} = \begin{bmatrix} \sigma_L^c \\ \sigma_T^c \\ \sigma_{LT}^c \end{bmatrix} + \begin{bmatrix} \rho_L f_L \\ \rho_T f_T \\ 0 \end{bmatrix}$   |  | (1) |
| $\begin{bmatrix} \sigma_L^c \\ \sigma_T^c \\ \tau_{LT}^c \end{bmatrix} = \begin{bmatrix} \cos^2(\alpha_D) & \sin^2(\alpha_D) & 2 \sin(\alpha_D) \cos(\alpha_D) \\ \sin^2(\alpha_D) & \cos^2(\alpha_D) & -2 \sin(\alpha_D) \cos(\alpha_D) \\ -\sin(\alpha_D) \cos(\alpha_D) & \sin(\alpha_D) \cos(\alpha_D) & \cos^2(\alpha_D) - \sin^2(\alpha_D) \end{bmatrix} \begin{bmatrix} \sigma_D \\ \sigma_R \\ 0 \end{bmatrix}$   |  | (2) |
| $\begin{bmatrix} \sigma_L \\ \sigma_T \\ \tau_{LT} \end{bmatrix} = \begin{bmatrix} \cos^2(\alpha_D) & \sin^2(\alpha_D) & 2 \sin(\alpha_D) \cos(\alpha_D) \\ \sin^2(\alpha_D) & \cos^2(\alpha_D) & -2 \sin(\alpha_D) \cos(\alpha_D) \\ -\sin(\alpha_D) \cos(\alpha_D) & \sin(\alpha_D) \cos(\alpha_D) & \cos^2(\alpha_D) - \sin^2(\alpha_D) \end{bmatrix} \begin{bmatrix} \sigma_D \\ \sigma_R \\ 0 \end{bmatrix} + \begin{bmatrix} \rho_L f_L \\ \rho_T f_T \\ 0 \end{bmatrix}$ |  | (3) |
| $\sigma_L = \sigma_D \cos^2(\alpha_D) + \rho_L f_L$   |  | (4) |
| $\sigma_T = \sigma_D \sin^2(\alpha_D) + \rho_T f_T$   |  | (5) |
| $\tau_{LT} = -\sigma_D \sin(\alpha_D) \cos(\alpha_D)$   |  | (6) |
| Compatibility equations (strains)   |  |     |
| $\begin{bmatrix} \epsilon_L \\ \epsilon_T \\ \gamma_{LT} \end{bmatrix} = \begin{bmatrix} \cos^2(\alpha_D) & \sin^2(\alpha_D) & 2 \sin(\alpha_D) \cos(\alpha_D) \\ \sin^2(\alpha_D) & \cos^2(\alpha_D) & -2 \sin(\alpha_D) \cos(\alpha_D) \\ -2 \sin(\alpha_D) \cos(\alpha_D) & 2 \sin(\alpha_D) \cos(\alpha_D) & 2 \cos^2(\alpha_D) - \sin^2(\alpha_D) \end{bmatrix} \begin{bmatrix} \epsilon_D \\ \epsilon_R \\ 0 \end{bmatrix}$   |  | (7) |
| $\epsilon_L + \epsilon_T = \epsilon_D + \epsilon_R$   |  | (8) |
| $\gamma_{LT} = 2(\epsilon_R - \epsilon_D) \sin(\alpha_D) \cos(\alpha_D)$  |  | (9) |

It should be noted that the initial estimates to initialize the solution procedure are computed using the Mohr compatibility truss model (MCTM) [9].

TABLE 2: Constitutive relationships for the materials [5–7].

| Concrete in compression  |  |
|--|--|
| $\sigma_D = \begin{cases} \zeta f_C' \left[ 2 \left( \frac{\epsilon_D}{\zeta \epsilon_0} \right) - \left( \frac{\epsilon_D}{\zeta \epsilon_0} \right)^2 \right], & \text{para } \epsilon_D \leq \zeta \epsilon_0 \\ \zeta f_C' \left[ 1 - \left( \frac{\frac{\epsilon_D}{\zeta \epsilon_0} - 1}{\frac{4}{\zeta} - 1} \right)^2 \right], & \text{para } \epsilon_D > \zeta \epsilon_0 \end{cases} \quad (10)$ |  |
| $\zeta = \frac{R(f_c')}{\sqrt{1 + \frac{400\epsilon_R}{\eta'}}} \quad (11)$  |  |
| $\eta = \frac{\rho_T f_{Ty}}{\rho_L f_{Ly}} \quad (12)$  |  |
| $\begin{cases} \eta \leq 1 \Rightarrow \eta' = \eta \\ \eta > 1 \Rightarrow \eta' = \frac{1}{\eta} \end{cases} \quad (13)$   |  |
| $R(f_c') = \frac{5,8}{\sqrt{f_c' (\text{MPa})}} \leq 0,9 \quad (14)$   |  |
| Reinforcement in tension   |  |
| $f_S = \begin{cases} E_S \epsilon_S & \text{for } \epsilon_S \leq \epsilon_n \\ f_{Sy} [(0,91 - 2B) + (0,02 + 0,25B) \frac{\epsilon_S}{\epsilon_{Sy}}] & \text{for } \epsilon_S > \epsilon_n \end{cases} \quad (15)$   |  |
| $\epsilon_n = (0,93 - 2B) \epsilon_{Sy} \quad (16)$  |  |
| $B = \frac{1}{\rho} \left( \frac{f_{cr}}{f_{Sy}} \right)^{1,5} \quad (17)$   |  |
| $f_{cr} = 0,311 \sqrt{f_{cr}' (\text{MPa})} \quad (18)$  |  |

## 2.2. Solution procedure

Based on recent works, which aimed to refine the RA-STM, an efficient algorithm was successfully developed and proposed [4–7]. The associated flow chart is illustrated in Fig. 2. This algorithm needs to be implemented in a computer. In previous studies, MATLAB packages were used to implement the solution procedure [6, 7].

## 3. Comparative Analysis with Some Experimental Results

Table 4 presents the main properties of two RC panels tested under shear and found in the literature [10, 11]. Some of the experimental results of these panels are compared below with those computed with the refined RA-STM [6, 7].

TABLE 3: Set of equations for the refined RA-STM [5–7]

| Proportional loading   |      |
|--|------|
| $\sigma_L = m_L \sigma_1$ (19) $\sigma_T = m_T \sigma_1$   | (20) |
| $\tau_{LT} = m_{LT} \sigma_1$  | (21) |
| $\sigma_1 = \frac{\sigma_L + \sigma_T}{2} + \sqrt{\left(\frac{\sigma_L + \sigma_T}{2}\right)^2 + \tau_{LT}^2}$   | (22) |
| $m_L \sigma_1 - \rho_L f_L = \sigma_D \cos^2(\alpha_D)$  | (23) |
| $m_T \sigma_1 - \rho_T f_T = \sigma_D \sin^2(\alpha_D)$  | (24) |
| $m_{LT} \sigma_1 = -\sigma_D \sin(\alpha_D) \cos(\alpha_D)$  | (25) |
| $\sigma_1 = \frac{1}{2A'} \left( B' \pm \sqrt{B'^2 - 4A'C'} \right)$   | (26) |
| $A' = m_L m_T - m_{LT}^2$  | (27) |
| $B' = m_L \rho_T f_T - m_T \rho_L f_L$   | (28) |
| $C' = \rho_T f_T \rho_L f_L$   | (29) |
| Relations between stresses and strains   |      |
| $f_L = \frac{m_L + m_{LT} \cot(\alpha_D)}{\rho_L} \sigma_1$  | (30) |
| $f_T = \frac{m_T + m_{LT} \tan(\alpha_D)}{\rho_T} \sigma_1$  | (31) |
| $\sigma_D = \frac{-m_{LT}}{\sin(\alpha_D) \cos(\alpha_D)} \sigma_1$  | (32) |
| $\epsilon_L = \frac{m_L + m_{LT} \cot(\alpha_D)}{E_S \rho_L} \sigma_1$   | (33) |
| $\epsilon_T = \frac{m_T + m_{LT} \tan(\alpha_D)}{E_S \rho_T} \sigma_1$   | (34) |
| $\epsilon_D = \frac{-m_{LT}}{E_c \sin(\alpha_D) \cos(\alpha_D)} \sigma_1$  | (35) |
| Residual function for MCTM   |      |
| $F_{MCTM} = \frac{\epsilon_L - \epsilon_D}{\epsilon_T - \epsilon_D} - \tan^2(\alpha_D) = 0$  | (36) |
| Residual function for RA-STM   |      |
| $F_{RA-STM} = \begin{bmatrix} \sigma_D \frac{\epsilon_T - \epsilon_D}{\epsilon_R - \epsilon_D} - m_L \sigma_1 + \rho_L f_L \\ \sigma_D \frac{\epsilon_L - \epsilon_D}{\epsilon_R - \epsilon_D} - m_T \sigma_1 + \rho_T f_T \end{bmatrix} = \begin{bmatrix} 0 \\ 0 \end{bmatrix}$ | (37) |

$$*\eta = \frac{\rho_T f_{Ty}}{\rho_L f_{Ly}}$$

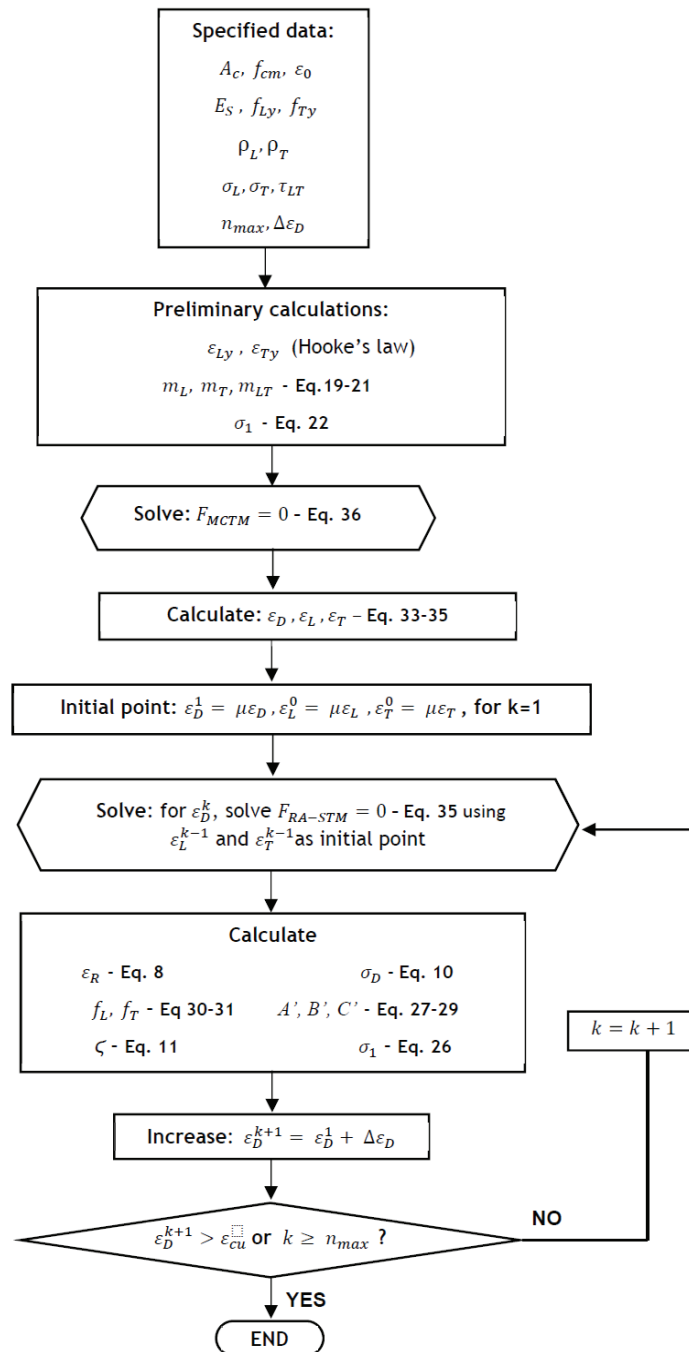


Figure 2: Flow Chart.

Fig. 3 shows the  $\sigma_D - \epsilon_D$  curves for concrete in compression (in the principal direction of compressive stresses) for panel VA1 [10]. Two curves are presented, the experimental one and the theoretical one computed from the refined RA-STM.

For the theoretical curve, a first stage with a quasi linear behaviour is observed. In this stage, as the compressive stress increases the corresponding strain also increases but at smaller rates. When the reinforcement yields, a strong nonlinear behaviour is

TABLE 4: Properties of tested RC panels under shear.

| Panel    | Concrete          |                     | Steel                  |               |                   |                      |               |                   | $\eta^*$ |
|----------|-------------------|---------------------|------------------------|---------------|-------------------|----------------------|---------------|-------------------|----------|
|          | $f_{cm}$<br>(MPa) | $\epsilon_0$<br>(‰) | Longitudinal direction |               |                   | Transverse direction |               |                   |          |
|          |                   |                     | $\rho_L$               | Reinforc.     | $f_{Ly}$<br>(MPa) | $\rho_T$             | Reinforc.     | $f_{Ty}$<br>(MPa) |          |
| VA1 [10] | 95,1              | 2,45                | 0,012                  | 10M@94<br>mm* | 445               | 0,012                | 10M@94<br>mm* | 445               | 1        |
| B2 [11]  | 44,1              | 2,35                | 0,0179                 | -             | 446               | 0,0119               | -             | 463               | 0,69     |

observed until the peak stress is reached. After this, the strains highly increase with a small variation of the compressive stresses. The panel continues to behave in this way until the criterion which define the theoretical failure is reached (at least one of the materials reach its conventional strain failure).

In the experimental graph, a first stage is also observed in which the compressive stress increases linearly with the corresponding strains, this latter at smaller rates. When the compressive stress reaches approximately 4,4 MPa, a slight decrease of the stiffness, as well as a sudden increase of the strain, is observed. This point of the graph corresponds to the cracking of the panel. After this, a second stage is observed, for which the compressive stress increases with the corresponding strains, this latter again at smaller rates, until the yielding of the reinforcement. In the third stage the strains highly increase and the compressive stress slowly decreases until failure is reached.

In general, the main features of the compressive concrete behaviour are well captured by the theoretical model, as well as the peak stress of concrete. However, the theoretical model is not able to predict the transition from the cracked stage to the uncracked stage. This is because the refined RA-STM neglects the influence of concrete in tension in the perpendicular direction to the principal compressive stresses ( $\sigma_R = 0$ , see Fig. 1 (b)), The previous results show that concrete in tension is important to be considered for low loading levels. In fact, the refined RA-STM considers that the plate is already fully cracked since the beginning of the loading. This simplification constitutes a drawback of the model, which needs to be solved because the transition from the cracked stage to the uncracked stage is important to be correctly predicted in order to assess the panel for loading services.

Fig. 4 shows the shear ( $\tau_{LT}$ ) versus shear strain ( $\gamma_{LT}$ ) curves, both experimental and theoretical, for panel B2 [11]. The dashed curve corresponds to the prediction from the refined RA-STM, while the continuous curve corresponds to the original RA-STM from Pang and Hsu in 1995 [11]. This latter accounts for the tensile strength of concrete,

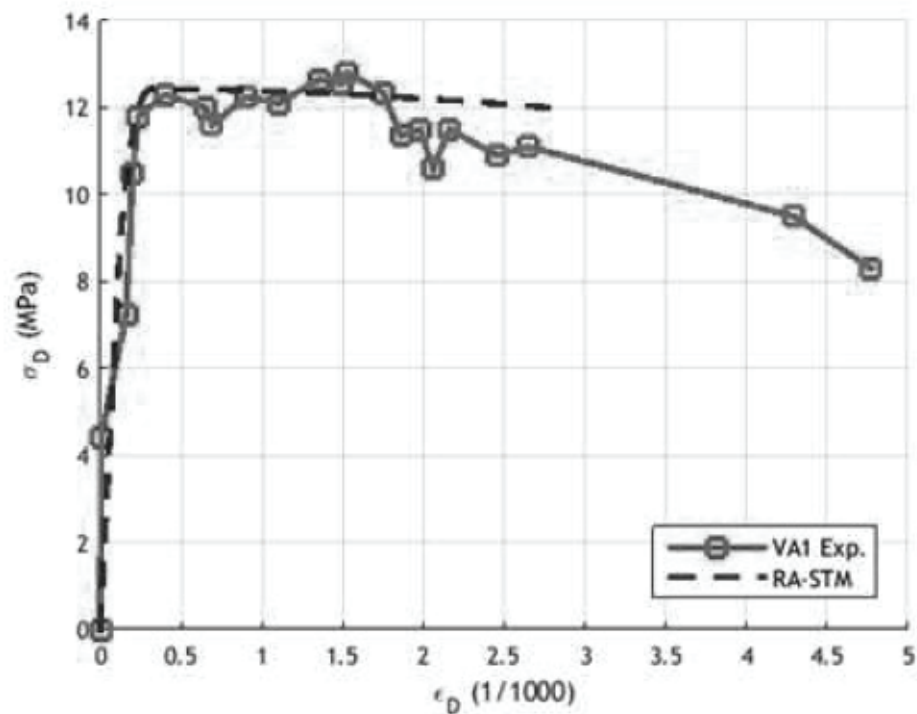


**Figure 3:** Comparison between  $\sigma_D - \epsilon_D$  curves for panel VA1 [10].

in opposition to the refined RA-STM. Fig. 4 shows that the original RA-STM captures better the behaviour of the panel for low loading levels. This shows the importance for the model to include the influence of the concrete in tension. For the ultimate stage, the refined RA-STM shows better agreement with the experiment curve. In Fig. 4, both versions of the theoretical model capture well another feature of panel B2. This panel is not reinforced symmetrically (see parameter  $\eta$  in Table 3), its transverse reinforcement ratio is lesser than its longitudinal reinforcement ratio. For this reason, both reinforcements (longitudinal and transverse) didn't yield for the same strain. This is shown in the graphs by two distinct points for which it is possible to observe two consecutive losses of stiffness, corresponding to the yielding of the transverse reinforcement (firstly) and longitudinal reinforcement (latter). This shows that RA-STM model is able to capture well the nonlinear behaviour under shear of asymmetrically reinforced panels.

#### 4. Future Developments for the Refined RA-STM

The previously presented results, related with panels VA1 and B2, generally show that the refined RA-STM is able to capture well the general features of panels under shear,

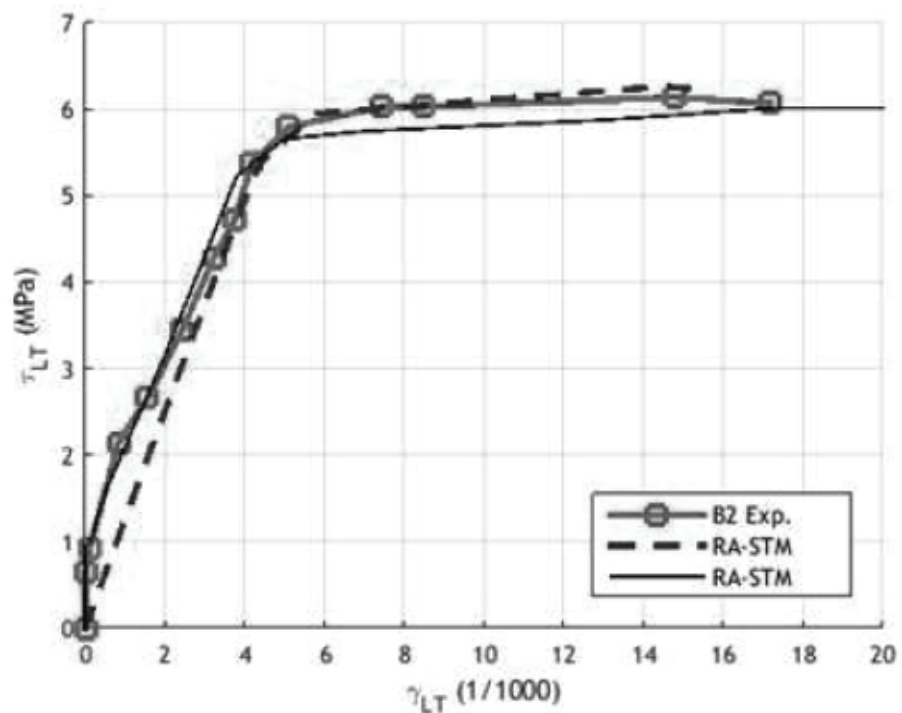


**Figure 4:** Comparison between  $\tau_{LT} - \gamma_{LT}$  curves for panel B2 [11].

namely for the ultimate stage. Additional examples with other panels under shear can be found in previous studies [6, 7], including for prestressed panels [8].

As referred before, the refined RA-STM neglects the influence of concrete in tension in the perpendicular direction to the principal compressive stresses. This drawback needs to be solved because the transition from the cracked stage to the uncracked stage needs to be correctly predicted. This is because current codes of practice impose to assess structural members for both the ultimate and service loading. For this latter, it is important to check the cracking load, as well as the stress state in the materials and the stiffness of the member after cracking.

The previous discussion only involved the behaviour of panels under shear. However, other loading conditions, such as axial stresses (combined or not with shear stresses) are common in structures (see Fig. 1 (a)). Few previous studies using RA-STM are focused on such condition loadings. Some of them show that RA-STM still do not capture the real behaviour of such panels and numerical problems are observed, which are mainly related with errors in the convergence criteria [6]. This shows that the RA-STM model still needs to be improved and generalized to other and more realistic loading conditions.

Finally, the intrinsic nonlinear feature of the RA-STM leads to a complex solution procedure, as previously shown. This problem can probably be minimized if the set of

equations are rewritten using other criteria, such as the energetic ones. Many problems in physics are more easily formulated if they are based on energetic criteria, regardless of how they are applied (minimization of the potential energy or principle of virtual work for static or pseudo-static systems, least action principle for dynamics systems, etc.). The application of energetic criteria to establish the solution procedure for the RA-STM is still an open issue.

The previous discussion shows that the refined RA-STM still need further developments.

## 5. Conclusions

This article presented a recent softened truss model with variable angle, namely the refined RA-STM, to model the behaviour of structural concrete membranes under pure shear. The equations, as well as the solution procedure of the model, were summarily presented. Some predictions from the refined RA-STM, related to panels tested under shear, were also presented and compared with the corresponding experimental results which were found in the literature. From the comparative analysis, it was shown that the general features of RC panels under shear are well captured by the refined RA-STM, namely for the ultimate stage. For low loading conditions, the need to refine the model was also shown. In addition, some ideas were discussed in order to justify future developments for the refined RA-STM. Such developments constitute the main objectives for the Ph.D. project of the first author, which include specifically the following ones:

- to unify the refined RA-STM for reinforced concrete and prestressed concrete membranes;
- to consider the influence of concrete in tension in the refined RA-STM through the incorporation of an additional average constitutive relationship in the calculation procedure;
- to generalize the refined RA-STM to other loading conditions, including shear combined with axial forces and also cyclic loading;
- to optimize and simplify the calculation procedure of the refined RA-STM by using energetic criteria.

Finally, it should be referred that experimental data related with structural concrete membranes are still scarce and are not sufficient to fully assess the reliability of the refined RA-STM. For this reason, additional numerical results based on calibrated models using FEM will certainly be useful.



## Notation

$E_s$  = Young's modulus for steel

$F_{MCTM}$  = residual function for MCTM

$F_{RA-STM}$  = residual function for RA-STM

$f'_c; f_{cm}$  = uniaxial compressive strength of concrete

$f_{cr}$  = tensile strength of concrete

$f_L$  = tensile stress in the longitudinal reinforcement

$f_{Ly}$  = yielding stress of the longitudinal reinforcement

$f_S$  = average tensile stress in the steel bars

$f_{sy}$  = yielding stress of the steel bars

$f_T$  = tensile stress in the transverse reinforcement

$f_{Ty}$  = yielding stress of the transverse reinforcement

$k$  = number of solution points

$m_L$  = longitudinal proportionality coefficient

$m_{LT}$  = shear proportionality coefficient

$m_T$  = transverse proportionality coefficient

$n_{max}$  = maximum number of solution points

$\alpha_D$  = angle of the principal compressive stresses in the concrete membrane element

$\alpha_R$  = angle of the principal tensile stresses in the concrete membrane element

$\epsilon_0$  = strain correspondent to the peak stress

$\epsilon_{cu}$  = ultimate strain for concrete in compression

$\epsilon_s$  = average strain in the steel bars

$\epsilon_{sy}$  = yielding strain of the steel bars

$\epsilon_D$  = principal average compressive strain

$\epsilon_L$  = longitudinal average strain

$\epsilon_R$  = principal average tensile strain

$\epsilon_T$  = transversal average strain

$\gamma_{LT}$  = average shear strain  $\zeta$  = softening coefficient

$\rho_L$  = longitudinal reinforcement ratio

$\rho_T$  = transverse reinforcement ratio

$\sigma_1$  = principal tensile stress in the RC membrane element

$\sigma_D$  = principal compressive strain in the concrete membrane element

$\sigma_L$  = longitudinal normal stress in the RC membrane element

$\sigma_L^c$  = longitudinal normal stress in the concrete membrane element

$\sigma_R$  = principal tensile strain in the concrete membrane element

$\sigma_T$  = transverse normal stress in the RC membrane element

$\sigma_T^c$  = transverse normal stress in the concrete membrane element  $\tau$  shear stress

$\tau_{LT}$  = shear stress in the RC membrane element

$\tau_{LT}^c$  = shear stress in the concrete membrane element

## References

- [1] MathWorks. (2017). "MATLAB - R2017". Academic license.
- [2] Belarbi A, Hsu TTC. Constitutive laws of concrete in tension and reinforcing bars stiffened by concrete. *Struct J Am Concr Inst.* 1994;91(4): 465–474.
- [3] Pang XB, Hsu TTC. Behavior of reinforced concrete membrane elements in shear. *Struct J Am Concr Inst.* 1995;92(6):665–679.
- [4] Silva JRB, Horowitz B. Efficient procedure to estimate the load–deformation behavior of reinforced concrete panels under membrane forces [in Portuguese]. CILAMCE 2015: Iberian Latin American Congress on Computational Methods in Engineering; 2015; Rio de Janeiro-RJ, Brazil; vol. 36.
- [5] Silva JRB. Efficient procedure for the analysis of reinforced concrete sections using the softened truss model [unpublished master's thesis]. Recife, Brazil: Department of Civil Engineering, Federal University of Pernambuco; 2016.
- [6] Cerquido BMD. Analysis of reinforced concrete sections with the softened truss model [unpublished master's thesis]. Covilhã, Portugal: Department of Civil Engineering and Architecture, University of Beira Interior; 2017.
- [7] Bernardo LFA, Cerquido BMD, Silva JRB, Horowitz B. Efficient Refined Rotating-Angle Softened Truss Model Procedure to Analyze Reinforced Concrete Membrane Elements. *Struct Concr. fib* 2018;19(6): 1971-1982.
- [8] Bernardo L, Lyrio A, Silva J, Horowitz B. Refined Softened Truss Model with Efficient Solution Procedure for Prestressed Concrete Membranes. *J Struct Eng ASCE.* 2018;144(6): 04018045.
- [9] Collins MP. Torque-twist characteristics of reinforced concrete beams. Inelasticity and non-linearity and non-linearity in structural concrete. Waterloo: University of Waterloo Press, 1973; p. 211–231.



- [10] Zhang LX, Hsu TTC. Behavior and analysis of 100 MPa concrete membrane elements. *J Struct Eng ASCE*. 1998;124(1):24–34.
- [11] Pang XB, Hsu TTC. Behavior of reinforced concrete membrane elements in shear. *Struct J Am Concr Inst*. 1995;92(6):665–679.